Turkish Journal of Physics

Volume 26 | Number 1 Article 6

1-1-2002

Kinetics of Light-induced Metastable Defect Creation and Annealing in a-Si:H

ALP OSMAN KODOLBAŞ

AYNUR ERAY

ÖZCAN ÖKTÜ

Turk J Phys
26 (2002) , 33 – 39.

Kinetics of Light-induced Metastable Defect Creation and Annealing in a-Si:H

Alp Osman KODOLBAŞ*, Aynur ERAY, Özcan ÖKTÜ
Hacettepe University, Department of Physics Engineering,
TR-06532 Beytepe, Ankara-TURKEY
e-mail: kodolbas@hacettepe.edu.tr

Received 26.01.2001

Abstract

Constant Photocurrent Method (CPM) and steady state photoconductivity measurements are used to investigate the creation of light-induced metastable defects in a-Si:H at room temperature and their annealing. Light-induced metastable defect concentration N_d varies with exposure time t_e as t_e^r with r=0.34±0.02, as expected from the recombination induced weak bond breaking model [1]. The validity of a stretched exponential model is also studied [2]. From the annealing experiments, the distribution of thermal annealing activation energies is calculated following the method proposed by Hata and Wagner [3]. Defects created at room temperature show a narrow distribution of annealing activation energies peaking at 0.97eV. The relation between photoconductivity and N_d is strongly nonlinear. Defects created at earlier times of illumination degrade photoconductivity more strongly, and these defects anneal out more easily than those created at later times of illumination.

Key Words: a-Si:H, Staebler-Wronski effect, Light induced metastable defect, CPM, Photoconductivity, Distribution of annealing activation energies.

1. Introduction

Light induced degradation in a-Si:H, also know as the Staebler–Wronski effect, [4] has been extensively studied since its discovery (see [5-6] and references therein). Despite the large number of studies in the pursuit of understanding reversible light-induced metastable changes in hydrogenated amorphous silicon (a-Si:H), the microscopic mechanism for the degradation is still controversial and some basic concepts remain confusing. Many microscopic models have been proposed [5], two of which have been widely accepted. In the first of these models, it is assumed that some of the weak bonds in amorphous silicon network are adjacent to the Si-H bond. Non-radiative recombination of photo carriers trapped in localised tail states leads to the breaking of weak Si-Si bonds. Hydrogen atom metastabilises the two resulting dangling bonds by bond switching [1]. In the second model, defect creation is related to a dispersive process, which slows down the creation rate and results in saturation at long exposure times [2]. This leads to a stretched exponential dependence of the defect density upon exposure time:

$$N(t) = N_S - (N_S - N_0)\exp(-(t/\tau)^{\beta}), \tag{1}$$

where N_0 and N_S are the initial and saturated density of defects respectively; β is given by the ratio T/T_0 where T_0 is the characteristic temperature of valance band tail; and τ is an effective time constant for the process.

*Corresponding author.

CPM is a simple and widely used method for measuring the subgap optical absorption coefficient α_{CPM} to determine ΔN_d, and this method is frequently employed to study light-induced metastable defect kinetics [6,7]. In our previous work, we have investigated the creation and annealing of light induced defects at 120K and briefly compared the results with those created at room temperature [7,8]. In the present paper, we present a detailed study on the creation and annealing kinetics of light induced defects in a-Si:H at room temperature by photoconductivity and CPM measurements. From the annealing experiments, we have calculated the distribution of annealing activation energies for the metastable defects created at 300K. One of the main aims was to study the relationship between photoconductivity and light induced defect density as a function of illumination intensity.

2. Experimental Details

Device-quality a-Si:H samples with thickness of about 1.5 μm prepared on Corning 7059 glass substrates are provided by ENEA Research Centre, Portici, Italy. Selected physical parameters of the sample used in the experiments are given in Table 1.

Table 1. Some selected parameters of the a-Si:H samples used in the experiment; d, thickness, [H] atomic hydrogen concentration, $\sigma_{AM1.5}/\sigma_d$, ratio of the photocurrent to the dark current under AM1.5 illumination, σ_0,minimum metallic conductivity, E_a, dark conductivity activation energy, E_g^T, Tauc gap, E_0, Urbach parameter, N_{d0}, density of dangling bond defects determined by 300K CPM. (*) Indicates the parameters provided by the ENEA research centre.

D(μm)	**[H] at. % (*)**	$\sigma_{AM1.5}/\sigma_d$ **(*)**	$\sigma_0(\Omega\mathbf{cm})^{-1}$	$\mathbf{E}_a$**(eV)**	$\mathbf{E}_g^T$**(eV)**	$\mathbf{E}_0$**(meV)**	$\mathbf{N}_{d0}$ **(cm^{-3})**
1.45	6-7	1.44x10^5	324	0.85±0.05	1.72±0.04	56±2	1.7x10^{16}

Optical absorption measurements were first performed to determine absorption coefficients and Tauc gap. For CPM and photoconductivity measurements, coplanar silver painted electrodes were formed at the top of the films to provide a 1x10 mm gap cell. For light-induced metastable defect creation, IR filtered light from a tungsten halogen lamp was used. The intensity of the light was calibrated with a small photodiode. The sample was kept in a homemade liquid N_2 flow cryostat during light-exposure steps and the tendency of the temperature increments were controlled by changing the liquid nitrogen flow rate. After each illumination step the decay of the photocurrent was monitored for 1 hour before CPM was measured at room temperature. All CPM measurements for different light exposed and annealed states were taken using the same constant photocurrent value, optimised for the most degraded state. Before any set of kinetic measurements, the sample was annealed at 415K for 1 h. The deep defect density (N_d) of various light exposed and annealed states were determined from the room temperature CPM absorption coefficient at 1.2 eV assuming $\alpha_{CPM}(1.2\text{ eV}) = 1\text{cm}^{-1}$, corresponding to a defect density of 2.5x10^{16} cm^{-3}[9]. Following CPM measurements, photoconductivity was measured at constant photon flux of 3 x 10^{13}photons/cm^{2}s using a LED group whose peak wavelength is 660 nm.

3. Results

The CPM spectra of the sample in the annealed state, together with CPM spectra measured after different light exposure times at 105 mW/cm^2 illumination, are shown in Fig. 1. All CPM spectra's are matched to the room temperature optical transmission measurements in the usual manner. To find the $\alpha_{CPM}(1.2\text{ eV})$ value for various light exposure times, corresponding spectra are smoothed using FFT methods.

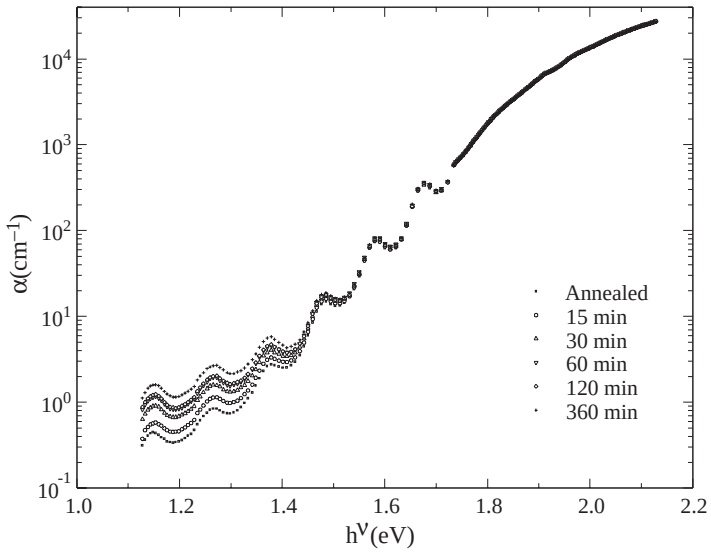

Figure 1. CPM spectra of the annealed sample and a set of CPM spectra measured at 300 K after different exposure durations. Sample was illuminated with 105 mW/cm^2 white light. Exposure durations are labelled in the figure.

The relative increase in subgap absorption $[\alpha(t_e)\text{-}\alpha(0)]/\alpha(0)$ for two different illumination intensities (55 mW/cm^2 and 105 mW/cm^2) are plotted as a function exposure time t_e in Fig. 2. The measured slopes agree both with the generally observed $t^{1/3}$ dependence of metastable defect creation and with the predictions of the weak bond-breaking model [1]. We also tried to fit the degradation data given in Fig. 2 with the stretched exponential dependence of the defect density with exposure time [2] given in Equation 1. For this calculation one needs to know the saturation value of the defect density. We did not try to reach saturation of light induced defect density. Light induced defect density in good quality undoped a-Si:H saturates at about 1-3x10^{17} cm^{-3}[5]. Due to low light intensity we used in comparison with those studies, we choose N_s=1x10^{17}cm^{-3}. A good fit was obtained for $\beta \cong 0.45 \pm 0.01$ with τ light intensity dependent: τ=4.1x10^{3}s for 55 mW/cm^2 and τ=3.2 x10^{4}s for 105 mW/cm^2 illuminations.

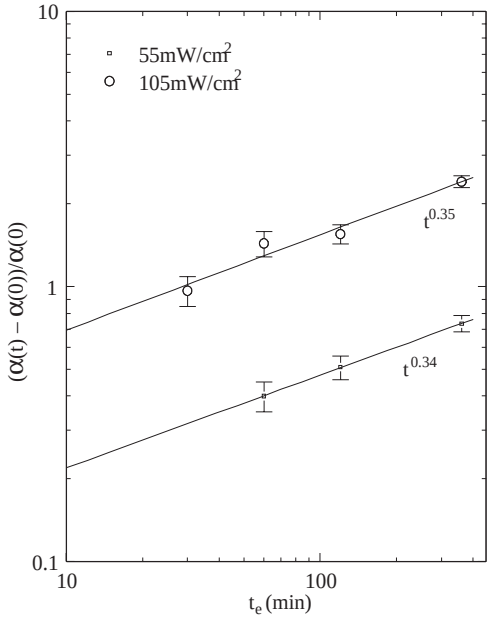

Figure 2. Relative increase in subgap absorption $[\alpha(t) - \alpha(0)]/\alpha(0)$ with exposure time t_e.

To study the annealing kinetics of light-induced defects after 6 h prolonged illumination using 55 mW/cm^2 intense light, we have carried out the following experiment. The sample was heated to annealing temperature T_A at a rate of about 5 K/min, kept at T_A for annealing time t_A and then cooled back to illumination temperature at a rate of about 5 K/min, with CPM were measured at room temperature. The annealing times and annealing temperatures were chosen to be 15 and 120 min at 373 K and 180 min at 393 K. The results are presented in Fig. 3. Defects created at room temperature using 55 mW/cm^2 light starts annealing above 360 K and above this temperature the annealing rate was very high.

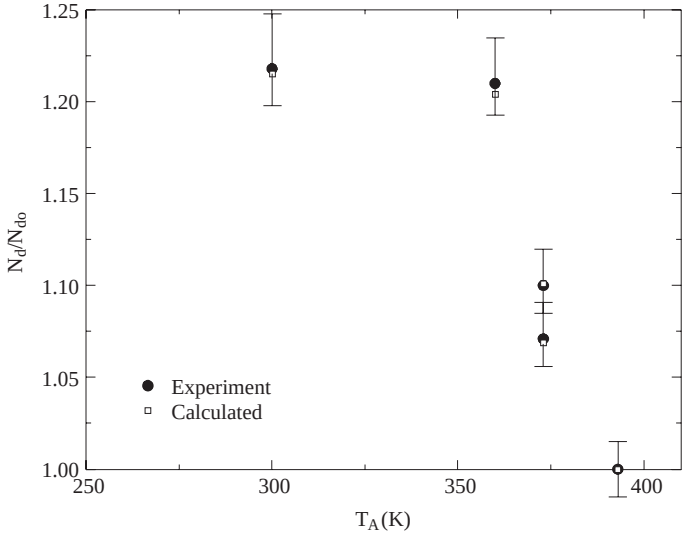

Figure 3. Normalized density of defects as a function of annealing temperature for the defects created after illuminating the sample with 55 mW/cm^{2}at 300 K.

Distribution of annealing activation energies must be considered in analysing the data presented in Fig. 3. Distribution of annealing activation energies can be obtained by assuming the view of Hata and Wagner [3], where annealing time rate of change of light induced metastable defects at annealing temperature T_A are proportional to their density $\Delta N_d(E_A, T_A, t)$, ie.,

$$\frac{d[\Delta N_d(E_A, T_A, t)]}{dt} = -\frac{\Delta N_d(E_A, T_A, t)}{\tau(E_A)}. \tag{2}$$

In this equation, $\tau(E_A)$ is the annealing time constant of defects and increases exponentially with the annealing activation energy as

$$\tau(E_A) = \tau_0 e^{\frac{E_A}{kT}}. \tag{3}$$

τ_0 is assumed to be constant at 1x10^{-10}s [3]. If the annealing activation energy distribution of the defects just after the cessation of light could be estimated then total light induced defects remaining after annealing at temperature T_A for time t_A could be calculated and fitted to the experimental data given in Fig. 3. At each annealing step total density of light-induced defects are calculated using the relation

$$\Delta N_d(T_A, t) = \int_0^\infty \Delta N_d(E_A, T = 300K, t = 0) e^{-\frac{t}{\tau_0 e^{(E_A/kT)}}} dE_A. \tag{4}$$

A very good match to experimental values is obtained if we take a narrow Gaussian distribution peaking at 0.97 eV as shown in Fig. 4. Evolution of defect density during annealing steps is also indicated in the Figures.

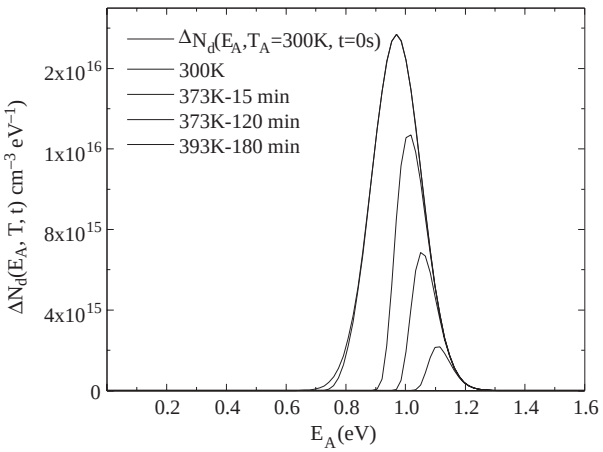

Figure 4. Distribution of annealing activation energies of photocreated defects in the as light soaked state at room temperature (solid line), and at various annealed states (dashed lines)

Once the annealing data, such as shown in Fig. 3, is obtained, the above mentioned calculation method leads to an almost unique distribution function for the metastable defect annealing activation energies: one cannot fit the experimental data shown in Fig. 3 to a distribution of a different character than the one presented in Fig. 4. Gaussian distribution is chosen for mathematical simplicity. It is possible that appreciable annealing of metastable defects might have taken place during the heating and cooling cycles and this extra annealing was estimated and added to the indicated errors on the experimental points of Fig. 3.

Light-induced metastable defects are believed to be better recombination centers than native defects [6]. In order to understand how the light induced defect density affects the photoconductivity, relative changes in the inverse $\mu\tau$-product as a function of relative changes in the subgap absorption coefficient at photon energy 1.2eV [α_{CPM}(1.2ev)] were plotted in Fig. 5 during 6 h degradation and successive annealing. The values of these quantities of the annealed sample are used for normalization. The upper parts of the curves are obtained with increasing exposure times while lower are determined for annealing at each consecutive step (degradation and annealing paths are described by arrows on the figure). No annealing data is present for 105 mW/cm^2 illumination. If there were a single valued relationship between defect concentration and photoconductivity then all the points should fall onto the same line. However, light induced degradation and annealing paths are different forming hysteresis-like changes [6]. Despite the large differences in defect concentration after 6 h illumination, 55 mW/cm^2 illumination degrades the photoconductivity as effectively as 105 mW/cm^2 illumination. Light induced local annealing of defects may be responsible for this observation [6].

4. Discussion

Weak bond-Dangling bond conversion was mostly assumed to be the origin of light induced metastable defects [5]. For example, in one of the most thoughtful models, weak bond breaking model, non-radiative recombination of photo-carriers trapped in localized tail states lead to the breaking of weak Si-Si bonds. H movement stabilizes the resulting dangling bonds by bond switching. If light induced defects orients from breaking of weak Si-Si bonds than one expects tail states to be reformed during intense illumination which is not in agreement with previous low temperature photoconductivity and subgap absorption measurements [6,10]. Our results presented in Fig. 1 are in agreement with those studies where upon illumination those tail and dangling bond states below 1.55 eV changes.

From the results presented in Fig. 2 we observe that defect creation efficiency is independent of light intensity used for the degradation and is given by exponent $t_e^{1/3}$ in accord with both previous studies [5, 6] as well as the weak bond breaking model [1]. On the other hand, defect creation rate is found to be strongly illumination intensity dependent. Light intensity dependence of metastable defect density was not one of

the aims of the present work. Validity of stretched exponential model was also tested, and our results are in agreement with previous studies [2].

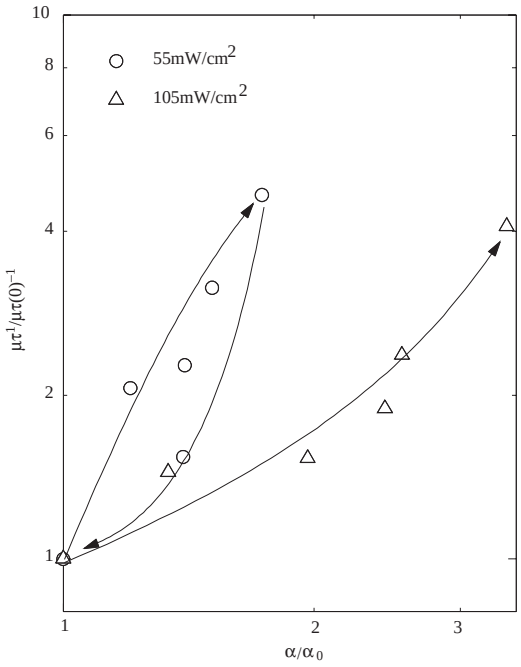

Figure 5. Relative change of inverse $\mu\tau$ product [$\mu\tau$ $^{-1}$] as a function of relative change in subgap absorption for 1.2 eV photon energy for two different illumination intensities.

Defects created at room temperature are found to be stable below about 360K. However, annealing rate is very high above this temperature. Complete annealing was achieved at 393K. Distribution of annealing activation energies has been calculated to analyze this observation. For the defects created at room temperature Stutzmann et al [1] evaluated that the return from the metastable to the stable state occurs over a barrier with thermal activation energy of about 1.1 eV [1]. Peak value of this barrier has been confirmed by subsequent studies [5 and the references therein]. Our results support these previous observations in that a narrow Gaussian distribution of annealing activation energies peaking at 0.97 eV describes the annealing of the defects created at 300K.

There is no single valued relationship between light-induced defect density and photoconductivity. Defects created at earlier times of illumination degrade photoconductivity more strongly, and these defects anneal out more easily than those created at later times of the illumination. Although more defects were created by 105 mW/cm^2 illumination than 55 mW/cm^2 illumination, photoconductivity decreases to about same value. Light induced local annealing of defects may be responsible for this observation [6].

5. Conclusion

We have investigated the creation of light induced defects at room temperature and their annealing. Light induced defect density increases with exposure time in agreement with weak bond breaking model.

Defects created at room temperature starts annealing above 360K and the annealing rate is very high above this temperature. The distribution of annealing activation energies, calculated to quantify this observation is a narrow Gaussian function peaking at 0.97eV and is in accord with previous studies [5, 9].

The relation between light-induced defect density and $\mu\tau$-product is strongly non-linear and for the present study depends on light intensity used for the degradation. Defects created at earlier times of illumination degrade photoconductivity more strongly, and these defects anneal out more easily than those created at later times of the illumination [6, 12].

Acknowledgements

The authors would like to thank G. Nobile from the ENEA Research Centre, Portici, Italy for kindly providing the samples.

References

[1] M. Stutzmann, W.B.Jackson and C.C.Tsai, *Phys. Rev.* **B,32(1)** (1985) 23.

[2] R. H. Bube, L. Echeverria and D. Redfield, *Appl. Phys. Lett.,* **57** (1990) 79.

[3] N. Hata and S. Wagner, *J. Appl. Phys.,* **72(7)** (1992) 2857.

[4] D. L. Staebler and C. R. Wronski, *Appl. Phys. Lett.* **31** (1977) 292.

[5] M. Stutzmann, *Mater. Res. Soc. Symp. Proc.* **467** (1997) 37.

[6] H. Fritzsche, *Mater. Res. Soc. Symp. Proc.* 467 (1997) 19.

[7] A. O. Kodolbaş, A. Eray, Ö. Öktü, *Journal of Non-Cryst. Solids*, **255** (1999) 132-139.

[8] A. O. Kodolbaş, A. Eray, Ö. Öktü, G. Nobile, "Thin Film Materials and Devices Development in Science and Technology", Proceedings of the Tenth International School on Condensed Matter Physics, Varna (1999) 445-448, Editors: J.M. Marshall, N. Kirov, A. Vavrek.

[9] N. Wyrsch, F. Finger, T. J. McMahon, M. Vanecek, *J. Non-Cryst. Solids* **137-138** (1991) 347.

[10] A. O. Kodolbaş, A. Eray, H. Tolunay, T. Güngör, G.J. Adriaenssens, Ö. Öktü, "Electronic, Optoelectronic and Magnetic Thin Films", Proc. of the Eighth International School on Condensed Matter Physics, Varna, (1994) 644, Editor J.M. Marshall, N. Kirov, A. Vavrek.

[11] Q. Zhang, H. Takashima, M. Kumeda and T. Shimuzu, *J. Non-Cryst. Solids* **198-200** (1996) 495.

[12] A. O. Kodolbaş, A. Eray, Ö. Öktü, *Solar Energy Materials and Solar Cells*, **69(4)** (2001) 325.